

# Modulation of surface reactivity via electron confinement in metal quantum well films: O<sub>2</sub> adsorption on Pb/Si(111)

Zhen Zhang,<sup>1</sup> Yanfeng Zhang,<sup>2</sup> Qiang Fu,<sup>1</sup> Hui Zhang,<sup>1</sup> Yunxi Yao,<sup>1</sup> Teng Ma,<sup>1</sup> Dali Tan,<sup>1</sup> Qikun Xue,<sup>2</sup> and Xinhe Bao<sup>1,a)</sup>

<sup>1</sup>State Key Laboratory of Catalysis, Dalian Institute of Chemical Physics, Chinese Academy of Sciences, Dalian 116023, People's Republic of China

<sup>2</sup>Department of Physics, Tsinghua University, Beijing 100084, People's Republic of China

(Received 4 February 2008; accepted 11 April 2008; published online 1 July 2008)

Pb quantum well films with atomic-scale uniformity in thickness over macroscopic areas were prepared on Si(111)-7×7 surfaces. As a probe molecule, O<sub>2</sub> was used to explore the effect of electron confinement in the metal films on the surface reactivity. X-ray photoelectron spectroscopy results showed clear oscillations of oxygen adsorption and Pb oxidation with the thickness of the Pb films. The higher reactivity to O<sub>2</sub> on the films with 23 and 25 ML Pb has been attributed to their highest occupied quantum well states being close to the Fermi level ( $E_F$ ) and the high density of the electron states at  $E_F$  (DOS- $E_F$ ), as evidenced by the corresponding ultraviolet photoelectron spectroscopy. A dominant role of DOS- $E_F$  was suggested to explain the quantum modulation of surface reactivity in metal quantum well films. © 2008 American Institute of Physics. [DOI: 10.1063/1.2919992]

## I. INTRODUCTION

Ultrathin metal films may be used as well-defined model systems for studies in surface catalysis. In the two-dimensional (2D) catalyst systems, the film thickness, as the main tunable structural parameter, can be well controlled down to nanometer or atomic-layer scale such that unusual catalytic properties might appear due to a size confinement at the film thickness. For example, Au 1×3 bilayer film grown on a titania surface is an order of magnitude more active than monolayer (ML) and thick (>2 ML) Au films for catalytic oxidation of CO.<sup>1</sup> For Pb quantum well films (2–6 nm thick) grown on Si(111), a well-defined up-down oscillation with a period of 2 ML in the surface reactivity to O<sub>2</sub> has been reported.<sup>2</sup> The distinct thickness-dependent surface reactivity indicates that quantum size effects (QSEs), which have been almost exclusively discussed in zero dimensional nanoparticle catalyst systems, could also play an important role in the 2D nanofilm catalyst systems.

The most significant QSE in the 2D film catalyst systems is the electron confinement in the vertical direction of the thin films, forming quantum well states (QWSs).<sup>3,4</sup> QWSs induced modification of CO chemisorption on metal surface was demonstrated on the ultrathin Cu films grown on a fcc-Fe surface.<sup>5</sup> A pronounced effect of QWSs on the initial surface oxidation rate was observed for well ordered Mg films of up to 15 atomic layers grown on a W(110) substrate.<sup>6,7</sup>

More recently, Ma *et al.* have directly observed a quantum oscillation in surface chemical reactivities in the nano-sized Pb quantum well films grown on Si(111).<sup>2</sup> Films with several consecutive thicknesses, for example, 10–16 ML,

were obtained in a wedge-shaped flat-top Pb mesa. The amount of the surface adsorbed O<sub>2</sub> and the rate of surface oxidation exhibit a clear Pb thickness dependence, as revealed by scanning tunneling microscopy (STM). The determination of surface electronic structure of the Pb films by scanning tunneling spectroscopy confirmed that the quantum oscillation in surface reactivity originated from the QWSs of the Pb mesas.

Here, we present an investigation of the quantum modulation of surface reactivity using Pb quantum well films grown on Si(111) over a macroscopic area, which allows us to detect the surface properties by using conventional electron spectroscopies. The adsorption of O<sub>2</sub> on the Pb films was studied by x-ray photoelectron spectroscopy (XPS) rather than the local probe technique of STM. A clear oscillation in the surface reactivity with various Pb thicknesses on such macroscopic scale films was also observed, which was found to be well relevant to the variation of the position of the highest occupied QWS with respect to the Fermi level ( $E_F$ ). Based on the experimental data, the intrinsic electronic factors that determine the surface reactivity were discussed in detail.

## II. EXPERIMENTAL

The experiments were performed in an Omicron multi-probe surface analysis system, which was described elsewhere.<sup>8,9</sup> XPS data were acquired by using Mg  $K\alpha$  ( $h\nu = 1253.6$  eV) radiation with pass energy of the energy analyzer set at 30 eV. The spectra were calibrated with Ag 3d<sub>5/2</sub> peaked at 368.1 eV. Ultraviolet photoemission (UP) spectra were recorded at normal emission with He I radiation ( $h\nu = 21.2$  eV) and the spectra were calibrated with respect to  $E_F$  of Si(111)-7×7. Both XPS and ultraviolet photoemission spectroscopy (UPS) data were collected at 150 K. The STM

<sup>a)</sup>Author to whom correspondence should be addressed. Tel.: +86-411-84686637; fax: +86-411-84694447. Electronic mail: xhbao@dicp.ac.cn.

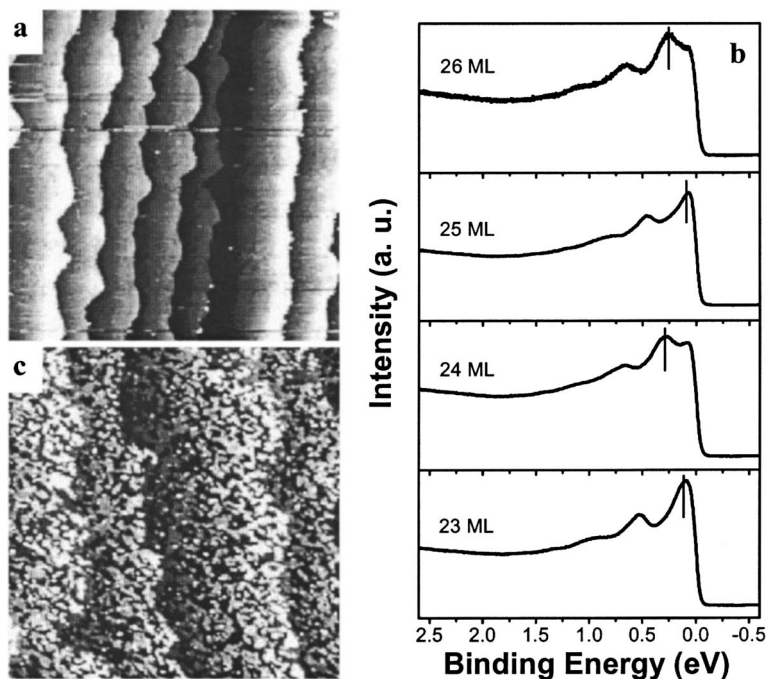


FIG. 1. (a) STM image of 23 ML Pb/Si(111), 2.6 V,  $1000 \times 1000 \text{ nm}^2$ . (b) UP spectra of 23, 24, 25, and 26 ML Pb/Si(111). (c) STM image of the 23 ML Pb/Si(111) after exposing 1140 L  $\text{O}_2$ , 2.4 V,  $500 \times 500 \text{ nm}^2$ .

measurement was carried out at room temperature (RT) with a constant current mode using a homemade W tip.

Si(111) surfaces were cleaned by flashing the samples to  $1200^\circ\text{C}$  for several cycles until the well-defined Si(111)- $7 \times 7$  reconstruction was observed by STM. A boron nitride crucible was used to produce Pb (purity 99.999%) atomic beams and the Pb flux was set at 0.3 ML/min. The atomically flat Pb films were prepared by depositing Pb onto Si(111)- $7 \times 7$  at 130 K and then annealing up to RT, which was called as a “two-step” growth method.<sup>10,11</sup>  $\text{O}_2$  was introduced onto the sample surfaces by backfilling the chamber via a leak valve while keeping the substrate at 150 K. In the text, the gas exposure is given in Langmuir (L),  $1 \text{ L} = 1 \times 10^{-6} \text{ Torr s}$ .

### III. RESULTS AND DISCUSSION

Using the two-step growth method,<sup>3,10,11</sup> atomically flat Pb quantum well films with the thicknesses of 23, 24, 25, and 26 ML were grown on Si(111) surfaces. As an example, Fig. 1(a) shows a typical STM image recorded from a 23 ML Pb film on Si(111) at RT and the surface is atomically flat with steps originated from the Si(111) substrate.<sup>3</sup> All of the Pb films present similar morphology having atomic-scale uniformity in thickness.

Free electrons in metal films grown on semiconductor substrate can be confined by the bandgap in the substrate and the image barrier at film-vacuum interface leading to the formation of discrete electronic states. The UP spectra acquired from the Pb/Si(111) surfaces at 150 K are displayed in Fig. 1(b) and discrete QWSs of the Pb films were observed near  $E_F$ . The observation of sharp and singular QWS peaks critically depends on the uniformity in the film thickness and flatness of the film surfaces.<sup>10</sup> The clear QWS peaks in the grown Pb films also indicate high quality of the prepared Pb quantum well films.

In metallic Pb films, the electron Fermi wavelength (1.06 nm) is about four times of the Pb interlayer spacing ( $2.85 \text{ \AA}$ ) along the crystallographic [111] direction such that the position of the highest occupied QWS should oscillate with respect to  $E_F$  between the odd and even layers.<sup>2,3,10</sup> Such an oscillation of the highest occupied QWS position [marked by short lines in Fig. 1(b)] with thickness has also been observed by our UPS experiments. The formation of QWSs will influence other surface electronic properties, such as surface work function, surface electronic density of states near  $E_F$  ( $\text{DOS}-E_F$ ), and decay of surface electronic density into vacuum.<sup>2,3,7,12-15</sup> Our data and the previous angle-resolved UPS (ARUPS) results<sup>3</sup> unambiguously demonstrate the modulation of  $\text{DOS}-E_F$  via thickness, i.e., higher  $\text{DOS}-E_F$  at the 23 and 25 ML Pb films but lower  $\text{DOS}-E_F$  at the 24 and 26 ML Pb films. Meanwhile, the surface work function is closely related to  $\text{DOS}-E_F$  and position of the highest occupied QWSs. In the case of QWS close to  $E_F$  and higher  $\text{DOS}-E_F$ , the electron states can tail into vacuum more strongly, which increases the surface dipole and, thereby, the surface work function.<sup>13,16</sup>

$\text{O}_2$  was chosen as the probe molecule to explore the surface reactivity of the Pb quantum well films with various thicknesses. It is found that the sticking probability of  $\text{O}_2$  on Pb surfaces is quite low above RT and the oxidation prefers to occur at the surface defect sites, such as steps and impurities.<sup>2,17</sup> Therefore, in the present work, the exposure of  $\text{O}_2$  to the Pb surfaces was preformed at 150 K. Figure 1(c) displayed a STM image of the 23 ML Pb/Si(111) film exposed to 1140 L  $\text{O}_2$  at 150 K and warmed up to RT. The Si-caused steps were still retained on the surface while the surface roughness increases due to the formation of some dendritic Pb oxide islands. The Pb oxide islands are homogeneously distributed on the surface and no preference at the steps was observed, which is in contrast to the Pb film oxidation at RT (Ref. 2) or elevated temperatures.<sup>17</sup> Upon  $\text{O}_2$

adsorption, the QWS peaks were strongly attenuated and almost disappeared after 1140 L O<sub>2</sub> exposure, which is due to a decrease in the surface uniformity by the formation of surface Pb oxide islands.

Figure 2 shows the Pb 4*f* (a) and O 1*s* (b) XP spectra from the 23 ML Pb/Si(111) film exposed to different amounts of O<sub>2</sub>. All of the O 1*s* peaks are located at 529.1 eV, the characteristic binding energy (BE) of atomic oxygen species, indicating the dissociative adsorption of O<sub>2</sub>.<sup>18,19</sup> The O 1*s* intensity keeps on increasing with O<sub>2</sub> adsorption and does not saturate even after an exposure of 1140 L O<sub>2</sub>. At the same time, the Pb 4*f* peaks become broad and asymmetric with shoulder peaks appeared at high BE. Deconvolution of the spectra produces two sets of peaks in each spectrum. For example, Pb 4*f* spectrum from the 23 ML Pb film exposed to 1140 L O<sub>2</sub> consists of Pb 4*f*<sub>7/2</sub> peaks at 136.9 and 138.0 eV, which correspond to Pb and PbO, respectively [shown in Fig. 2(c)].<sup>18,19</sup>

Both the O 1*s* intensity and the percentage of surface oxidized Pb can be used to characterize the surface reactivity of Pb films to O<sub>2</sub>. Figure 3(a) plotted the ratio of O 1*s* intensity to Pb 4*f* ( $I_{\text{O}}/I_{\text{Pb}}$ ) as a function of Pb film thickness at various O<sub>2</sub> exposures. The  $I_{\text{O}}/I_{\text{Pb}}$  values were higher for the 23 and 25 ML Pb films and a well-defined up-down oscillation of  $I_{\text{O}}/I_{\text{Pb}}$  with thickness can be clearly discriminated, which is particularly significant for large O<sub>2</sub> exposure. At the same time, the percentage of oxidized Pb component in Pb 4*f* signal ( $I_{\text{ox}}/I_{\text{total}}$ ) shows a similar dependence on Pb film thickness: on the surfaces of 23 and 25 ML Pb films, more Pb has been oxidized for 1140 L O<sub>2</sub> exposure while relatively weak Pb oxidation occurs on the 24 and 26 ML Pb films under the same adsorption conditions [Fig. 3(b)]. For comparison, the DOS- $E_F$  of the different Pb films determined by ARUPS (Ref. 3) was shown in Fig. 3(c).

The data in Fig. 3 distinctly show that O<sub>2</sub> adsorption and Pb oxidation are strongly dependent on the film thickness, and the 23 and 25 ML Pb films have higher reactivity to O<sub>2</sub> than the 24 and 26 ML films. In contrast to O<sub>2</sub> adsorption on the flat-top Pb islands consisting of films with several consecutive thicknesses, where the surface oxygen diffusion between the neighboring Pb films has to be taken into consideration, here O<sub>2</sub> was exposed to a macroscopic Pb film with single thickness and O<sub>2</sub> adsorption is solely determined by the surface property of the film. Furthermore, since the probe area of XPS is quite large (millimeter scale), the observed oscillating oxidation behavior is the intrinsic and macroscopic character of the Pb films. The present result is a complement to the previous work of Ma *et al.*,<sup>2</sup> both of which unambiguously show that O<sub>2</sub> adsorption on the surfaces of Pb quantum well films demonstrates a strong thickness dependence. Chemisorption properties of metal surfaces are usually determined by electronic and geometric factors, and both of them are often mixed together.<sup>20</sup> The Pb quantum well films on Si(111) have the same Pb(111) surface atomic structure and, thus, we can conclude that the modulation of oxygen adsorption on the Pb/Si(111) surfaces can be attributed to the different surface electronic structures. As discussed above, the thickness-dependent QWSs modulate the surface work function, surface DOS- $E_F$ , and the decay of

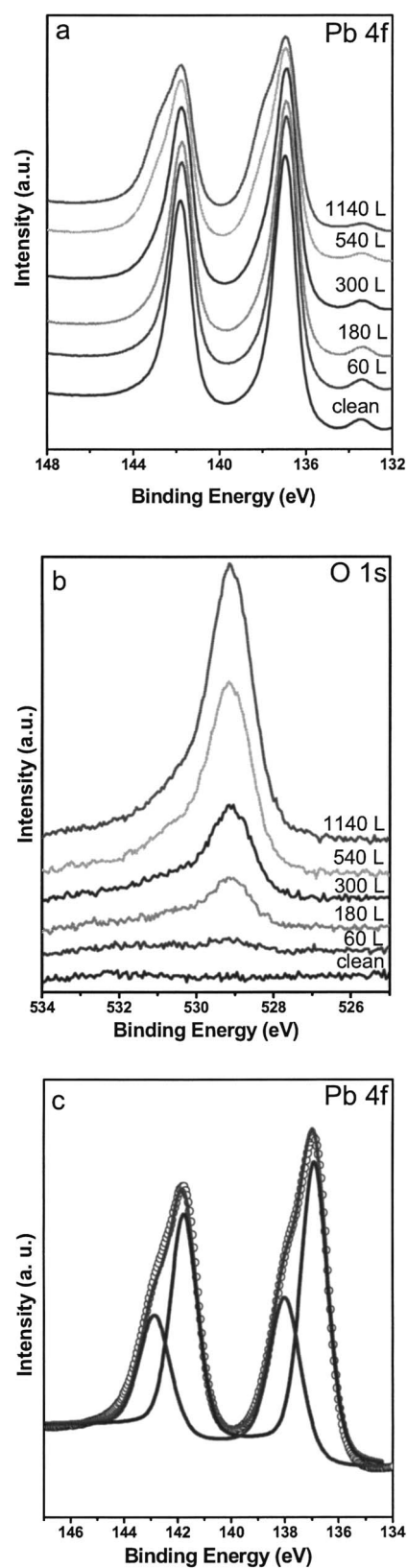


FIG. 2. Pb 4*f* (a) and O 1*s* (b) XP-spectra of 23 ML Pb/Si(111) surface with different O<sub>2</sub> exposures at 150 K. (c) The decomposition of Pb 4*f* of the 23 ML Pb/Si(111) after exposing 1140 L O<sub>2</sub>.

electronic density into vacuum. Their effects on the surface adsorption will be discussed in the following.

The dissociative adsorption of molecules on metal surfaces may take place through two dynamic processes: direct

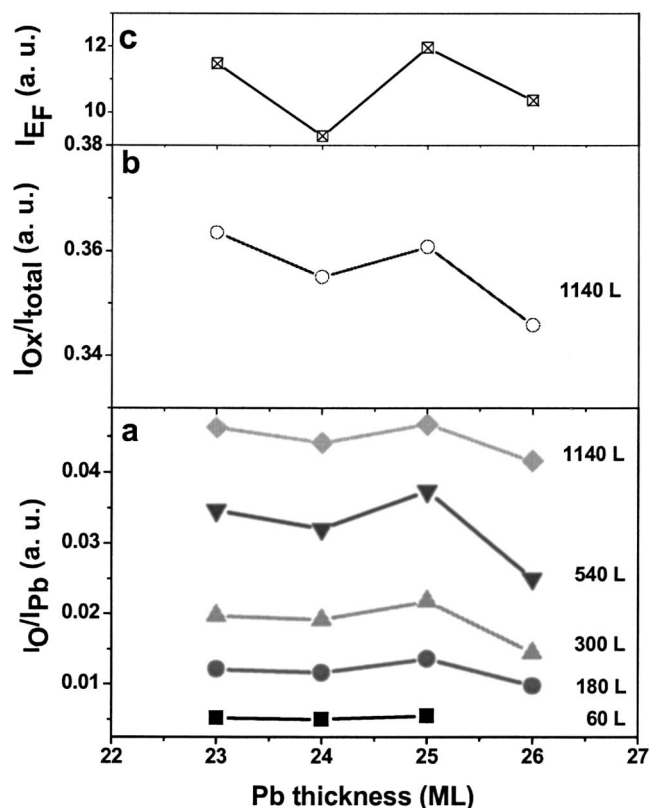


FIG. 3. (a) XPS intensity ratio of O 1s to Pb 4f ( $I_{O}/I_{Pb}$ ) of the Pb/Si(111) surfaces as a function of Pb film thickness at various oxygen exposure. (The  $O_2$  exposure has been indicated at the right part.) (b) The relative weight of Pb oxide component in Pb 4f spectra of the Pb/Si(111) surfaces ( $I_{Ox}/I_{total}$ ) at 1140 L  $O_2$  exposure. (c) The density of states (DOS) within 30 meV below  $E_F$  determined by ARUPS as a function of the Pb thin film thickness (from Ref. 3).

dissociation or indirect dissociation. For example,  $H_2$  and  $CH_4$  dissociate directly from the gas phase on some transition metal surfaces.<sup>21–23</sup> In the direct dissociation process, it is the Pauli repulsion between the occupied orbitals of adsorbate molecules and charge densities, in particular, the evanescent charge densities, in front of metal surfaces that contributes to physisorption potential and the change in activation energy barrier to dissociation. It has been found that the population of surface states or reduced surface work function enhances the Pauli repulsion and increases the barrier.<sup>23–26</sup> The same mechanism is also dominant in the physisorption of inert gases on metal surfaces.<sup>23,27</sup>

In contrast, the indirect dissociation necessitates an intermediate state through which a molecule passes before dissociation on a surface, and a molecularly chemisorbed state is often regarded as the precursor to the dissociation (marked as  $X_2^*$  in Fig. 4). This molecularly chemisorbed precursor mechanism applies to dissociation adsorption of  $O_2$ ,  $N_2$ , CO, and NO on many metal surfaces.<sup>22,28–34</sup> Although there is no detailed study in  $O_2$  adsorption on Pb surfaces, we suggest that this mechanism also dominates the  $O_2$  dissociation on Pb(111), which can be testified by the decrease in the sticking probability of oxygen on Pb(111) with the adsorption temperature increased from 100 K to RT.<sup>2</sup> The interaction between the molecular precursor and the metal surface determines the depth and shape of the molecular chemisorption

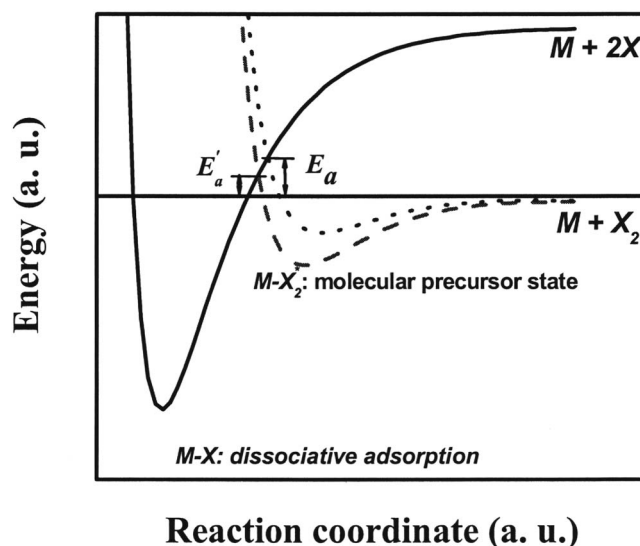


FIG. 4. Schematic one-dimensional potential energy diagram for molecular ( $X_2$ )-metal surface interaction. The electronic interaction between the molecularly chemisorbed precursor ( $M-X_2^*$ ) and the metal surface determines the depth and shape of the chemisorption well, and the energy barrier to dissociation adsorption ( $M-X$ ). Higher DOS- $E_F$  at metal surface favors the stronger molecule-surface bonding and the chemisorption well changes from the dotted line to the dashed line. Consequently, the energy barrier to the dissociation decreases from  $E_a$  to  $E_a'$ .

well, which may increase or decrease the activation barrier to dissociation (as shown in Fig. 4). Based on the classic forward-backward donation concept of metal-adsorbate bonding,<sup>35</sup> the bonding strength is mainly dependent on the charge transfer from metal surfaces to antibonding orbitals of molecular adsorbates. Various factors have been suggested to contribute to the electronic interaction between molecules and metal surfaces.

The surface work function, which is defined as the minimum energy needed to free an electron in the metal,<sup>36</sup> plays an important role in surface adsorption and reactions.<sup>32,37–41</sup> According to the Newns–Anderson adsorption model,<sup>42,43</sup> when a molecule, for example,  $O_2$ , approaches a jellium metal surface, the antibonding state  $\pi_g^*$  of the  $O_2$  molecule hybridizes with the  $sp$  band of the surface and broadens into a resonant state. The relative position of the broadened antibonding  $\pi_g^*$  resonance state with respect to  $E_F$  of the metal determines the charge transfer process. When the resonance state falls below  $E_F$ , electrons flow from the occupied states near  $E_F$  of the metal to the antibonding molecular orbital, which may lead to  $O_2$  dissociation. Therefore, it was proposed that a metal surface with lower surface work function could favor backdonation into the antibonding orbital and result in strong adsorbate adsorption on the surface. At a metal surface, electrons can spill out by tunneling into vacuum and the charge separation contributes to the formation of the surface dipole and surface work function.<sup>16,36</sup> For the Pb QW films, the film at the thickness with higher DOS- $E_F$  and the highest occupied QWS close to  $E_F$  will have a more significant electron spill out into the vacuum, which increases the surface dipole and thereby creates a larger work function. This was corroborated by the recent photoelectron spectroscopy experiments of Pb/Si(111)- $\sqrt{3}$

$\times \sqrt{3}$  surfaces<sup>13</sup> and density-functional calculations of free-standing Pb films.<sup>14</sup> Therefore, the 23 and 25 ML Pb films having higher DOS- $E_F$  [see Figs. 1(c) and 3(c)] present larger work functions. According to the adsorption model discussed above, the 23 and 25 ML Pb films should have a lower O<sub>2</sub> adsorption ability than the 24 and 26 ML Pb films, which conflicts the XPS results (Fig. 3). Therefore, the surface work function may not be the dominant factor in the observed quantum oscillation of O<sub>2</sub> adsorption on Pb quantum well films.

DOS at  $E_F$  of a metal surface is suggested to be another key factor in determining the surface reactivity.<sup>2,5,6,34,44–49</sup> For example, a linear relationship between the molecule adsorption energy and the surface DOS near  $E_F$  has been observed for NO adsorption on RhAg alloys<sup>34</sup> and CO adsorption on Pt catalysts.<sup>50–52</sup> The thickness-dependent oscillations in CO adsorption strength on Cu quantum well films,<sup>5</sup> oxidation rate of Mg quantum well films,<sup>6,49</sup> and oxidation rate of Pb quantum well films [Ref. 2 and Fig. 3 in the present work] are found to be governed by the oscillating changes in DOS- $E_F$ . The stronger surface adsorption or reaction is accompanied by higher DOS- $E_F$ . All these results indicate the important role of the surface DOS- $E_F$  in the metal-adsorbate interaction, which can be understood by the frontier-orbital theory.<sup>53</sup> The bonding of a molecule on a metal surface mainly relies on the interaction between the orbitals of the metal at  $E_F$  and the frontier orbitals of the molecule. The surface DOS- $E_F$  characterizes both the number of the metal's highest occupied molecular orbitals (HOMOs) that could give their electrons into the molecule's lowest unoccupied molecular orbital (LUMO) and the number of the metal's LUMOs that are ready to pull electrons out of the molecule's HOMO. An increase in the surface DOS- $E_F$  means a larger number of electrons that can be transferred from the metal surface to unoccupied orbitals of the adsorbate, which will enhance the back-donation interaction.

Besides the number of transferable electrons, the charge transfer rate is also critical in the metal-adsorbate electronic interaction. It has been proposed that the charge transfer occurs by electron tunneling.<sup>24,49,54–56</sup> In a charge transfer (CT) model, the CT rate through a resonance tunneling of a metal surface electron to antibonding orbital of the molecule is shown to be linearly proportional to DOS- $E_F$ .<sup>49,55</sup> Furthermore, the electron transfer rate via tunneling exponentially depends on decay length ( $\lambda$ ) in vacuum of the local DOS- $E_F$ . Recent theoretical and experimental results show that high surface DOS- $E_F$  corresponds to large decay length.<sup>7,15</sup> Thus, a surface with higher surface DOS- $E_F$  presents a higher CT rate between metal and adsorbate.

The present picture of DOS- $E_F$  could well explain the quantum modulation of surface reactivity in metal quantum well films. At thickness where the presence of an occupied QWS close to  $E_F$  enhances the DOS- $E_F$ , the metal surface presents a high density of transferable electrons and at the same time CT rate is high due to the large decay length of surface electronic density into vacuum. Both factors stabilize the molecularly chemisorbed precursor, for example, O<sub>2</sub><sup>\*</sup>, by the strong backdonation into antibonding orbitals of the molecule. As shown in Fig. 4, the strong bonding between the

molecular precursor and the metal surface deepens the molecular chemisorption well (changing from the dotted line to the dashed line) and, consequently, the barrier to dissociation decreases from  $E_a$  to  $E_a'$ . Therefore, adsorption and dissociation of molecules are facilitated on the surface.

#### IV. CONCLUSIONS

Pb quantum well films with atomic-scale uniformity in thickness over macroscopic areas have been prepared on Si(111)- $7 \times 7$  surfaces via a two-step growth process. Upon O<sub>2</sub> exposure to the Pb films, dissociative adsorption of oxygen, oxidation of the surface Pb, and formation of homogeneously distributed dendritic Pb oxide islands have been observed. The XPS results showed strong oscillations in the intensity of the surface adsorbed oxygen and the oxidation of the Pb surfaces with thickness of the Pb quantum well films. The 23 and 25 ML Pb films, of which the highest occupied QWSs are close to  $E_F$  and DOS- $E_F$  is high, have a higher reactivity to O<sub>2</sub> than the 24 and 26 ML films. High surface DOS- $E_F$  strengthens bonding of the molecularly adsorbed precursor on the metal surface and decreases the barrier to dissociation, facilitating the surface adsorption and reaction.

#### ACKNOWLEDGMENTS

This work was financially supported by the National Natural Science Foundation of China (NSFC, Nos. 20573107, 20603037, and 20733008), the Ministry of Science and Technology (MOST, No. 2007CB815200), and Chinese Academy of Sciences (CAS).

<sup>1</sup>M. S. Chen and D. W. Goodman, *Science* **306**, 252 (2004).

<sup>2</sup>X. C. Ma, P. Jiang, Y. Qi, J. F. Jia, Y. Yang, W. X. Duan, W. X. Li, X. H. Bao, S. B. Zhang, and Q. K. Xue, *Proc. Natl. Acad. Sci. U.S.A.* **104**, 9204 (2007).

<sup>3</sup>Y. Guo, Y. F. Zhang, X. Y. Bao, T. Z. Han, Z. Tang, L. X. Zhang, W. G. Zhu, E. G. Wang, Q. Niu, Z. Q. Qiu, J. F. Jia, Z. X. Zhao, and Q. K. Xue, *Science* **306**, 1915 (2004).

<sup>4</sup>T. C. Chiang, *Surf. Sci. Rep.* **39**, 181 (2000).

<sup>5</sup>A. G. Danese, F. G. Curti, and R. A. Bartynski, *Phys. Rev. B* **70**, 165420 (2004).

<sup>6</sup>L. Aballe, A. Barinov, A. Locatelli, S. Heun, and M. Kiskinova, *Phys. Rev. Lett.* **93**, 196103 (2004).

<sup>7</sup>N. Binggeli and M. Altarelli, *Appl. Phys. Lett.* **96**, 036805 (2006).

<sup>8</sup>Z. Zhang, Q. Fu, H. Zhang, Y. Li, Y. X. Yao, D. L. Tan, and X. H. Bao, *J. Phys. Chem. C* **111**, 13524 (2007).

<sup>9</sup>Z. Q. Jiang, W. X. Huang, Z. Zhang, H. Zhao, D. L. Tan, and X. H. Bao, *Surf. Sci.* **601**, 844 (2007).

<sup>10</sup>Y. F. Zhang, J. F. Jia, T. Z. Han, Z. Tang, Q. T. Shen, Y. Guo, Z. Q. Qiu, and Q. K. Xue, *Phys. Rev. Lett.* **95**, 096802 (2005).

<sup>11</sup>L. Y. Ma, L. Tang, Z. L. Guan, K. He, K. An, X. C. Ma, J. F. Jia, and Q. K. Xue, *Phys. Rev. Lett.* **97**, 266102 (2006).

<sup>12</sup>J. J. Paggel, C. M. Wei, M. Y. Chou, D. A. Luh, T. Miller, and T. C. Chiang, *Phys. Rev. B* **66**, 233403 (2002).

<sup>13</sup>P. S. Kirchmann, M. Wolf, J. H. Dil, K. Horn, and U. Bovensiepen, *Phys. Rev. B* **76**, 075406 (2007).

<sup>14</sup>C. M. Wei and M. Y. Chou, *Phys. Rev. B* **66**, 233408 (2002).

<sup>15</sup>Y. Qi, X. C. Ma, P. Jiang, S. H. Ji, Y. S. Fu, J. F. Jia, Q. K. Xue, and S. B. Zhang, *Appl. Phys. Lett.* **90**, 013109 (2007).

<sup>16</sup>N. D. Lang and W. Kohn, *Phys. Rev. B* **1**, 4555 (1970).

<sup>17</sup>K. Thürmer, E. Williams, and J. Reutt-Robey, *Science* **297**, 2033 (2002).

<sup>18</sup>R. W. Hewitt and N. Winograd, *Surf. Sci.* **78**, 1 (1978).

<sup>19</sup>*Handbook of X-ray Photoelectron Spectroscopy*, edited by J. F. Moulder, W. F. Stickle, P. E. Sobol, and K. D. Bpmben (Perkin Elmer, Eden Prairie, MN, 1992).

<sup>20</sup>J. R. Kitchin, J. K. Nørskov, M. A. Barteau, and J. G. Chen, *Phys. Rev.*

- Lett.* **93**, 156801 (2004).
- <sup>21</sup>W. Dong and J. Hafner, *Phys. Rev. B* **56**, 15396 (1997).
- <sup>22</sup>R. Schennach, G. Krenn, B. Klötzer, and K. D. Rendulic, *Surf. Sci.* **540**, 237 (2003).
- <sup>23</sup>E. Bertel and N. Memmel, *Appl. Phys. A: Mater. Sci. Process.* **63**, 523 (1996).
- <sup>24</sup>E. Bertel, P. Roos, and J. Lehmann, *Phys. Rev. B* **52**, R14384 (1995).
- <sup>25</sup>J. K. Brown, A. C. Luntz, and P. A. Schultz, *J. Chem. Phys.* **95**, 3767 (1991).
- <sup>26</sup>S. Yoneda, Y. Babasaki, M. Tanaka, F. H. Geuzebroek, F. Koga, N. Yamazaki, and A. Namiki, *Surf. Sci.* **363**, 11 (1996).
- <sup>27</sup>E. Bertel, *Surf. Sci.* **367**, L61 (1996).
- <sup>28</sup>A. Eichler, F. Mittendorfer, and J. Hafner, *Phys. Rev. B* **62**, 4744 (2000).
- <sup>29</sup>L. Vattuone, M. Rocca, C. Boragno, and U. Valbusa, *J. Chem. Phys.* **101**, 713 (1994).
- <sup>30</sup>A. Raukema, D. A. Butler, F. M. A. Box, and A. W. Kleyn, *Surf. Sci.* **347**, 151 (1996).
- <sup>31</sup>V. Zhukov, I. Popova, and J. T. Yates, Jr., *Surf. Sci.* **441**, 251 (1999).
- <sup>32</sup>G. Ertl, S. B. Lee, and M. Weiss, *Surf. Sci.* **114**, 527 (1982).
- <sup>33</sup>S. Kneitz, J. Gemeinhardt, and H.-P. Steinrück, *Surf. Sci.* **440**, 307 (1999).
- <sup>34</sup>O. R. Inderwildi, S. J. Jenkins, and D. A. King, *Surf. Sci.* **601**, L103 (2007).
- <sup>35</sup>G. Blyholder, *J. Phys. Chem.* **68**, 2772 (1964).
- <sup>36</sup>G. A. Somorjai, *Introduction to Surface Chemistry and Catalysis* (Wiley, New York, 1994).
- <sup>37</sup>C. G. Vayenas, S. Bebelis, and S. Ladas, *Nature (London)* **343**, 625 (1990).
- <sup>38</sup>C. G. Vayenas and D. Tsiplakides, *Surf. Sci.* **467**, 23 (2000).
- <sup>39</sup>H. P. Bonzel, *Surf. Sci. Rep.* **8**, 43 (1987).
- <sup>40</sup>U. Heiz, A. Sanchez, S. Abbet, and W. D. Schneider, *J. Am. Chem. Soc.* **121**, 3214 (1999).
- <sup>41</sup>J. K. Nørskov, S. Holloway, and N. D. Lang, *Surf. Sci.* **137**, 65 (1984).
- <sup>42</sup>D. News, *Phys. Rev.* **178**, 1123 (1969).
- <sup>43</sup>J. K. Nørskov, *Rep. Prog. Phys.* **53**, 1253 (1990).
- <sup>44</sup>M. H. Cohen, M. V. Ganduglia-Pirovano, and J. Kudrnovský, *Phys. Rev. Lett.* **72**, 3222 (1994).
- <sup>45</sup>M. Kulawik, H.-P. Rust, M. Heyde, N. Nilius, B. A. Mantoosh, P. S. Weiss, and H.-J. Freund, *Surf. Sci.* **590**, L253 (2005).
- <sup>46</sup>V. S. Stepanyuk, N. N. Negulyaev, L. Niebergall, R. C. Longo, and P. Bruno, *Phys. Rev. Lett.* **97**, 186403 (2006).
- <sup>47</sup>P. J. Feibelman and D. R. Hamann, *Phys. Rev. Lett.* **52**, 61 (1984).
- <sup>48</sup>P. J. Feibelman and D. R. Hamann, *Surf. Sci.* **149**, 48 (1985).
- <sup>49</sup>A. Hellman, *Phys. Rev. B* **72**, 201403R (2005).
- <sup>50</sup>Y. Y. Tong, P. Mériaudeau, A. J. Renouprez, and J. J. van der Klink, *J. Phys. Chem. B* **101**, 10155 (1997).
- <sup>51</sup>Y. Y. Tong, J. J. Billy, A. J. Renouprez, and J. J. van der Klink, *J. Am. Chem. Soc.* **119**, 3929 (1997).
- <sup>52</sup>Y. Y. Tong, C. Rice, N. Godbout, A. Wieckowski, and E. Oldfield, *J. Am. Chem. Soc.* **121**, 2996 (1999).
- <sup>53</sup>R. Hoffmann, *Rev. Mod. Phys.* **60**, 601 (1988).
- <sup>54</sup>M. Dean and M. Bowker, *Appl. Surf. Sci.* **35**, 27 (1988).
- <sup>55</sup>A. Hellman, B. Razaznejad, Y. Yourdshahyan, H. Ternow, I. Zorić, and B. I. Lundqvist, *Surf. Sci.* **532–535**, 126 (2003).
- <sup>56</sup>A. Hellman, B. Razaznejad, and B. I. Lundqvist, *Phys. Rev. B* **71**, 205424 (2005).